Vol. 37 (2006) ACTA PHYSICA POLONICA B No 12

GLOBAL VARIABLES FOR VARIOUS CENTRALITIES AT RHIC: A CRACOW MODEL APPROACH*

Dariusz Prorok

Institute of Theoretical Physics, University of Wrocław
Pl. Maksa Borna 9, 50-204 Wrocław, Poland

(Received October 3, 2006)

The final p_{T}-spectra measured at RHIC at $\sqrt{s_{NN}} = 130$ and $200\,\mathrm{GeV}$ are fitted within the Cracow single-freeze-out model. Then the global variables like the transverse energy at midrapidity, the charged particle multiplicity at midrapidity and the total multiplicity of charged particles are evaluated. The predictions agree fairly well with the experimental data. The centrality independence of the total number of charged particles per participant pair has been also reproduced.

PACS numbers: 25.75.–q, 25.75.Dw, 24.10.Pa, 24.10.Jv

1. The single-freeze-out model and global variable estimates

In this lecture the application of the single-freeze-out statistical model [1–5] to the final data on the p_{T} spectra of identified charged particles measured in the Relativistic Heavy Ion Collider (RHIC) at $\sqrt{s_{NN}} = 130$ and $200\,\mathrm{GeV}$ [6–12] is reviewed. Details of this analysis can be found elsewhere [13]. The foundations of the model are as follows: (a) the chemical and thermal freeze-outs take place simultaneously, (b) all confirmed resonances up to a mass of 2 GeV from the Particle Data Tables [14] are taken into account, (c) a freeze-out hypersurface is defined by the equation $\tau = \sqrt{t^2 - r_x^2 - r_y^2 - r_z^2} = \mathrm{const}$, ($d$) the four-velocity of an element of the freeze-out hypersurface is proportional to its coordinate, $u^\mu = x^\mu/\tau$, (e) the transverse size is restricted by the condition $r = \sqrt{r_x^2 + r_y^2} < \rho_{\max}$. The maximum transverse-flow parameter can be expressed as $\beta_\perp^{\max} = (\rho_{\max}/\tau)/(\sqrt{1 + (\rho_{\max}/\tau)^2})$. The model has four parameters, namely, the two thermal

* Presented at the XLVI Cracow School of Theoretical Physics, Zakopane, Poland May 27–June 5, 2006.

parameters, the temperature T and the baryon number chemical potential μ_B, and the two geometric parameters, τ and $\rho_{\rm max}$.

With the use of the following parametrization of the hypersurface

$$\begin{aligned} t &= \tau \cosh\alpha_{\parallel} \cosh\alpha_{\perp}\,, & r_x &= \tau \sinh\alpha_{\perp} \cos\phi\,, \\ r_y &= \tau \sinh\alpha_{\perp} \sin\phi\,, & r_z &= \tau \sinh\alpha_{\parallel} \cosh\alpha_{\perp}\,, \end{aligned} \tag{1}$$

the invariant distribution of the measured particles of species i can be expressed in the form

$$\frac{dN_i}{d^2p_{\rm T}\,dy} = \tau^3 \int\limits_{-\infty}^{+\infty} d\alpha_{\parallel} \int\limits_{0}^{\rho_{\rm max}/\tau} \sinh\alpha_{\perp} d(\sinh\alpha_{\perp}) \int\limits_{0}^{2\pi} d\xi\;(p\cdot u)\,f_i(p\cdot u)\,, \tag{2}$$

where

$$p\cdot u = m_{\rm T}\cosh\left(\alpha_{\parallel}-y\right)\cosh\alpha_{\perp} - p_{\rm T}\cos\xi\sinh\alpha_{\perp}\,, \tag{3}$$

and f_i is the final momentum distribution of the particle in question. The final distribution means here that f_i is the sum of primordial and simple and sequential decay contributions to the particle distribution (for details see [4, 15]).

Having integrated the distribution, Eq. (2), over $p_{\rm T}$ and summing over appropriate final particles, one can obtain transverse energy ($dE_{\rm T}/d\eta|_{\rm mid}$) and charged particle multiplicity ($dN_{\rm ch}/d\eta|_{\rm mid}$) densities at mid-rapidity (for details see [13]). The experimentally measured transverse energy is defined as

$$E_{\rm T} = \sum_{i=1}^{L} \hat{E}_i \cdot \sin\theta_i\,, \tag{4}$$

where θ_i is the polar angle, $\hat{E}_i$ denotes $E_i - m_N$ (m_N means the nucleon mass) for baryons, $E_i + m_N$ for antibaryons and the total energy E_i for all other particles, and the sum is taken over all L emitted particles [16, 17].

In the case of expansion satisfying the condition $d\sigma_\mu \sim u_\mu$ on a freeze-out hypersurface (as here), the total multiplicity of particle species i can be derived in the form

$$\begin{aligned} N_i &= \int d^2p_{\rm T}\,dy\,\frac{dN_i}{d^2p_{\rm T}\,dy} = \int d\sigma \int d^2p_{\rm T}\,dy\;(p\cdot u)\;f_i(p\cdot u) \\ &= \int d\sigma\; n_i(T,\mu_B) = n_i(T,\mu_B)\int d\sigma\,, \end{aligned} \tag{5}$$

if the local thermal parameters are constant on this hypersurface. The density n_i is not the primordial thermal density of particle species i but it collects also contributions from decays of resonances. The last integral in

Eq. (5) expresses the hypersurface volume and if the rapidity of the fluid element $\alpha_\parallel$ is unlimited (*cf.* Eq. (2)), then this volume will be infinite. Thus $\alpha_\parallel$ is assumed to have its maximal value $\alpha_\parallel^{\max}$. Then the volume can be expressed as $2\pi\ \alpha_\parallel^{\max}\tau\rho_{\max}^2$ and the total multiplicity of charged particles is obtained:

$$\begin{aligned} N_{\rm ch} &= 2\pi\ \alpha_\parallel^{\max}\tau\rho_{\max}^2 \sum_{i\in B} n_i(T,\mu_B) \\ &= 2\pi\ \alpha_\parallel^{\max}\tau\rho_{\max}^2\, n_{\rm ch}(T,\mu_B)\,, \end{aligned} \tag{6}$$

where $B=\{\pi^+,\pi^-,\,K^+,\,K^-,p,\,\bar{p}\}$. For $\alpha_\parallel^{\max}$ the following parametrization is obtained (for details see [13]):

$$\alpha_\parallel^{\max}(c) = y_{\rm p} - \frac{\langle\delta y\rangle}{0.975}\,(1-c)\,, \tag{7}$$

where $y_{\rm p}$ is the projectile rapidity, $\langle\delta y\rangle$ the average rapidity loss and c is a fractional number representing the middle of a given centrality bin, *i.e.* $c=0.025$ for the $0-5\%$ centrality bin, *etc.*

2. Results

Studies of the particle ratios and $p_{\rm T}$ spectra at various centralities in the framework of the single freeze-out model were done for the preliminary RHIC data at $\sqrt{s_{NN}} = 200$ GeV [18, 19] in [5]. The procedure has two stages. First, thermal parameters T and μ_B are fitted with the use of the experimental ratios of hadron multiplicities at midrapidity. After then two next parameters, τ and $\rho_{\max}$, are determined from the simultaneous fit to the transverse-momentum spectra of $\pi^\pm$, $K^\pm$, p and $\bar{p}$. Both fits are performed with the help of the χ^2 method. Since (a) the preliminary data for the $p_{\rm T}$ spectra [18, 19] differ from the final data [8, 9], (b) not all bins were fitted in [5], (c) the data points were digitized from the plots in [5], the fit procedure for determination of the geometric parameters of the model, τ and $\rho_{\max}$, has been performed again. For completeness the PHENIX case at $\sqrt{s_{NN}} = 130$ GeV has been repeated, since the first published data were for three bins only [6]. The data for the next two bins, which were not fitted in [4], were added in the later report [7]. Also the BRAHMS spectra measured at $\sqrt{s_{NN}} = 200$ GeV [10–12] have not been fitted within this model until now. The thermal parameters for the three cases of the maximal RHIC collision energy have been taken from the newer studies of the particle abundance ratios [20, 21].

The final results for the geometric parameters $\rho_{\max}$ and τ are gathered in Table I together with the corresponding values of $\beta_{\perp}^{\max}$ and χ^2/NDF for each centrality class characterized by the number of participants $N_{\rm part}$. All fits are statistically significant beside the most peripheral bins of the PHENIX measurements.

TABLE I

Values of the geometric parameters of the model fitted to the RHIC final data on the $p_{\rm T}$ spectra of identified charged hadrons [7–12]. Values of the thermal parameters are taken from the quoted references.

Collision case	$N_{\rm part}$	$\rho_{\max}$ [fm]	τ [fm]	$\beta_{\perp}^{\max}$	χ^2/NDF
PHENIX at	347.7	6.50 ± 0.27	8.23 ± 0.23	0.62	0.52
$\sqrt{s_{NN}} = 130$ GeV:	271.3	5.99 ± 0.21	7.29 ± 0.18	0.63	0.46
$T = 165$ MeV	180.2	5.08 ± 0.18	6.34 ± 0.15	0.63	0.49
$\mu_B = 41$ MeV	78.5	3.59 ± 0.15	4.81 ± 0.13	0.60	0.74
[1]	14.3	1.68 ± 0.19	3.14 ± 0.22	0.47	1.32
PHENIX at	351.4	8.46 ± 0.10	8.84 ± 0.08	0.69	0.80
$\sqrt{s_{NN}} = 200$ GeV:	299.0	7.99 ± 0.10	8.23 ± 0.08	0.70	0.61
$T = 155.2$ MeV	253.9	7.54 ± 0.10	7.67 ± 0.08	0.70	0.48
$\mu_B = 26.4$ MeV	215.3	7.11 ± 0.10	7.17 ± 0.07	0.70	0.48
[20]	166.6	6.45 ± 0.09	6.47 ± 0.07	0.71	0.58
	114.2	5.57 ± 0.08	5.63 ± 0.06	0.70	0.77
	74.4	4.68 ± 0.07	4.85 ± 0.06	0.69	1.05
	45.5	3.83 ± 0.07	4.16 ± 0.05	0.68	1.13
	25.7	2.99 ± 0.06	3.47 ± 0.05	0.65	1.41
	13.4	2.22 ± 0.06	2.78 ± 0.05	0.62	1.55
	6.3	1.71 ± 0.06	2.40 ± 0.05	0.58	1.40
STAR at	352	9.22 ± 0.18	7.13 ± 0.06	0.79	0.29
$\sqrt{s_{NN}} = 200$ GeV:	299	8.40 ± 0.17	6.83 ± 0.06	0.78	0.27
$T = 160.0$ MeV	234	7.57 ± 0.15	6.33 ± 0.06	0.77	0.23
$\mu_B = 24.0$ MeV	166	6.50 ± 0.14	5.86 ± 0.06	0.74	0.30
[21]	115	5.52 ± 0.12	5.37 ± 0.06	0.72	0.27
	76	4.66 ± 0.11	4.91 ± 0.06	0.69	0.27
	47	3.87 ± 0.10	4.40 ± 0.06	0.66	0.35
	27	3.07 ± 0.09	3.94 ± 0.06	0.61	0.46
	14	2.37 ± 0.08	3.32 ± 0.06	0.58	0.87
BRAHMS at	357	8.75 ± 0.16	8.38 ± 0.11	0.72	0.50
$\sqrt{s_{NN}} = 200$ GeV:	328	8.50 ± 0.15	8.08 ± 0.10	0.72	0.52
$T = 155.2$ MeV	239	7.52 ± 0.13	7.28 ± 0.09	0.72	0.46
$\mu_B = 26.4$ MeV	140	6.29 ± 0.12	6.20 ± 0.09	0.71	0.36
[20]	62	4.42 ± 0.12	4.95 ± 0.10	0.67	0.61

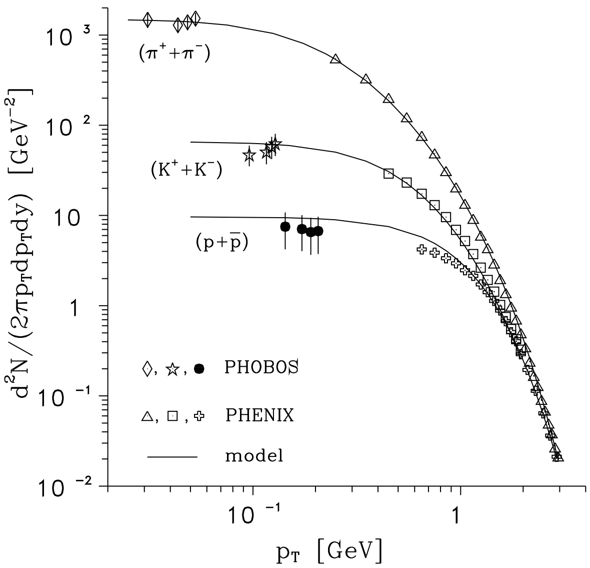

Fig. 1. Invariant yields as a function of p_T for RHIC at $\sqrt{s_{NN}} = 200$ GeV. The PHOBOS data are for the 15% most central collisions with the error bars expressed as the sum of the systematic and statistical uncertainties [22]. The corresponding PHENIX data are presented as the averages of the invariant yields for the 0–5 %, 5–10 % and 10–15 % centrality bins with no errors given. Lines are the appropriate predictions of the single-freeze-out model.

To check the accuracy of the model predictions, the invariant distributions given by Eq. (2) are calculated down to the low-p_T region (0.03–0.05 GeV for pions, 0.09–0.13 GeV for kaons and 0.14–0.21 GeV for protons and antiprotons) of the PHOBOS measurements at $\sqrt{s_{NN}} = 200$ GeV [22]. The results are depicted in Fig. 1. As one can see predictions agree very well with the low-p_T data.

In Fig. 2 predictions for $dN_{\rm ch}/d\eta|_{\rm mid}$ per participating pair as a function of centrality are presented for $\sqrt{s_{NN}} = 200$ GeV. In the STAR case results agree well with the data. In the PHENIX case results agree within errors with the data from the summing up of the integrated charged hadron yields [8], but they are significantly below the straightforward PHENIX measurements [17]. This reflects the observed discrepancy between the directly measured $dN_{\rm ch}/d\eta$ and $dN_{\rm ch}/d\eta$ expressed as the sum of the integrated charged hadron yields [18].

In Fig. 3 the estimates of $dE_{\rm T}/d\eta|_{\rm mid}$ per participating pair are shown as a function of centrality for $\sqrt{s_{NN}} = 200$ GeV. The predictions agree well with the data, only the most central point of the STAR case is substantially overestimated ($\approx 17\%$).

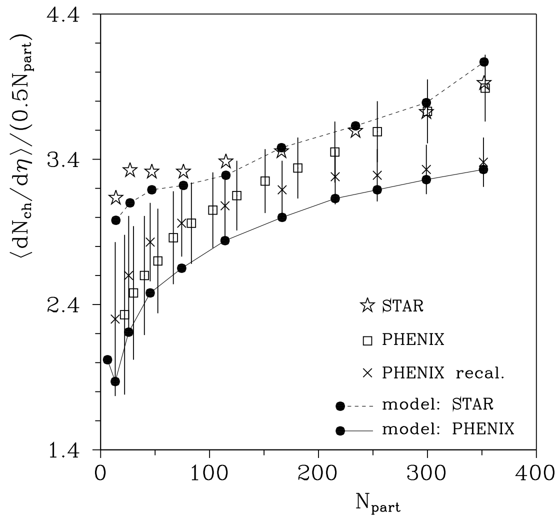

Fig. 2. $dN_{\mathrm{ch}}/d\eta$ per pair of participants *versus* N_{part} for RHIC at $\sqrt{s_{NN}} = 200$ GeV. The original PHENIX data are from [17], whereas the recalculated PHENIX data are from summing up the integrated charged hadron yields delivered in [8]. Also the STAR data are depicted with no errors given as in the source paper [9]. The lines connect the results and are to guide the eye.

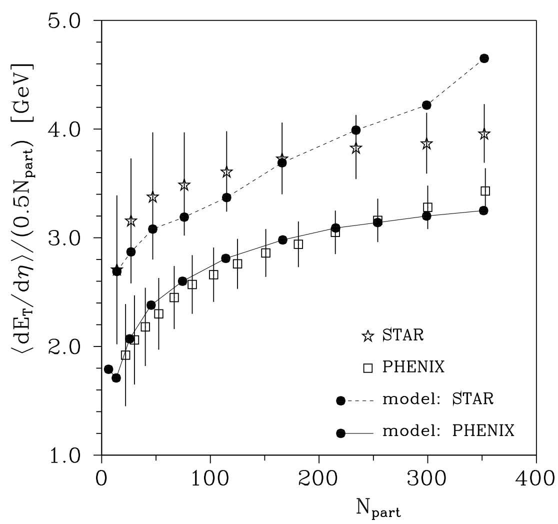

Fig. 3. $dE_{\mathrm{T}}/d\eta$ per pair of participants *versus* N_{part} for RHIC at $\sqrt{s_{NN}} = 200$ GeV. The PHENIX data are from [17] but the original STAR data from [16] have been rescaled to $\eta = 0$, see [13] for more explanations. The lines connect the results and are to guide the eye.

The predictions for the total charged-particle multiplicity per participating pair are presented in Fig. 4. One can see that estimated values are roughly constant within the range of the PHOBOS measurement [23], *i.e.* $N_{\rm part} \approx 60$–360. Only $\approx 10\%$ deviation from this constancy can be observed in the BRAHMS case. Also the predicted (absolute) values agree with the data within $\approx 10\%$.

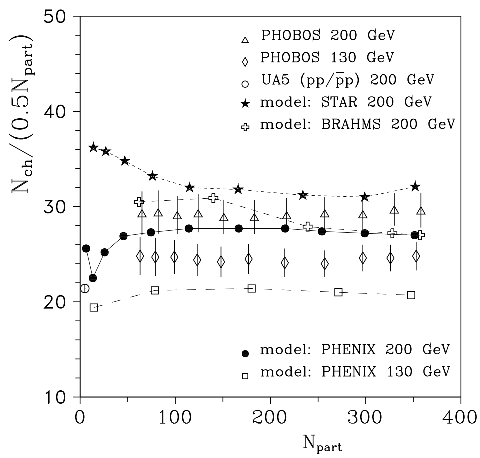

Fig. 4. $N_{\rm ch}$ per pair of participants *versus* $N_{\rm part}$ for RHIC at $\sqrt{s_{NN}} = 130$ and 200 GeV. The PHOBOS data are from [23] and the $pp/\bar{p}p$ data point of the UA5 measurement is from Fig. 39.5 in [14]. The lines connect the results and are to guide the eye.

3. Conclusions

Global variables like the transverse energy density, the charged particle multiplicity density and the total multiplicity of charged particles have been estimated in the framework of the single-freeze-out model for the Au–Au collisions at $\sqrt{s_{NN}} = 130$ and 200 GeV. The estimates are based on the fits of the parameters of the model which are done in the first stage. While the thermal parameters have been taken from independent fits to the particle yield ratios, the geometric parameters have been determined from the final data on the $p_{\rm T}$-spectra of identified charged hadrons. The consistent picture of the freeze-out has been obtained within the model since the global variables are measured independently of identified hadron spectroscopy and their predictions agree fairly well with the data. It should be stressed that the model reproduces the centrality independence of the total charged-particle multiplicity per participating pair and the predicted values agree with the measured ones within $\approx 10\%$. This is surprising since geometric parameters have been fitted to spectra measured at midrapidity, but the total charged-particle multiplicity is measured in the whole rapidity range.

The author would like to thank Jan Rafelski for very helpful comments and discussions. This work was supported in part by the Polish State Committee for Scientific Research (KBN) under contract No. KBN 2 P03B 069 25.

REFERENCES

[1] W. Florkowski, W. Broniowski, M. Michalec, *Acta Phys. Pol. B* **33**, 761 (2002).

[2] W. Broniowski, W. Florkowski, *Phys. Rev. Lett.* **87**, 272302 (2001).

[3] W. Broniowski, W. Florkowski, *Phys. Rev.* **C65**, 064905 (2002).

[4] W. Broniowski, A. Baran, W. Florkowski, *Acta Phys. Pol. B* **33**, 4235 (2002).

[5] A. Baran, W. Broniowski, W. Florkowski, *Acta Phys. Pol. B* **35**, 779 (2004).

[6] K. Adcox *et al.* [PHENIX Collaboration], *Phys. Rev. Lett.* **88**, 242301 (2002).

[7] K. Adcox *et al.* [PHENIX Collaboration], *Phys. Rev.* **C69**, 024904 (2004).

[8] S.S. Adler *et al.* [PHENIX Collaboration], *Phys. Rev.* **C69**, 034909 (2004).

[9] J. Adams *et al.* [STAR Collaboration], *Phys. Rev. Lett.* **92**, 112301 (2004).

[10] I. Arsene *et al.* [BRAHMS Collaboration], *Phys. Rev.* **C72**, 014908 (2005).

[11] I.G. Bearden *et al.* [BRAHMS Collaboration], *Phys. Rev. Lett.* **94**, 162301 (2005).

[12] I.G. Bearden *et al.* [BRAHMS Collaboration], *Phys. Rev. Lett.* **93**, 102301 (2004).

[13] D. Prorok, *Phys. Rev.* **C73**, 064901 (2006).

[14] K. Hagiwara *et al.* [Particle Data Group Collaboration], *Phys. Rev.* **D66**, 010001 (2002).

[15] D. Prorok, *Eur. Phys. J.* **A24**, 93 (2005).

[16] J. Adams *et al.* [STAR Collaboration], *Phys. Rev.* **C70**, 054907 (2004).

[17] S.S. Adler *et al.* [PHENIX Collaboration], *Phys. Rev.* **C71**, 034908 (2005) [Erratum-ibid. **C71**, 049901 (2005)].

[18] T. Chujo [PHENIX Collaboration], *Nucl. Phys.* **A715**, 151 (2003) and `http://alice-france.in2p3.fr/qm2002/Transparencies/20Plenary/Chujo.ppt`.

[19] O. Barannikova, F. Wang [STAR Collaboration], *Nucl. Phys.* **A715**, 458 (2003).

[20] J. Rafelski, J. Letessier, G. Torrieri, *Phys. Rev.* **C72**, 024905 (2005).

[21] O. Barannikova [STAR Collaboration], *J. Phys. G* **31**, S93 (2005).

[22] B.B. Back *et al.* [PHOBOS Collaboration], *Phys. Rev.* **C70**, 051901(R) (2004).

[23] B.B. Back *et al.* [PHOBOS Collaboration], `nucl-ex/0301017`.